

# EFFECT OF GRAIN SIZE AND PREFERRED CRYSTAL TEXTURE ON ACOUSTIC PROPERTIES OF 304 STAINLESS STEEL

N. Grayeli, F. Stanke, G. S. Kino, and J. C. Shyne  
Edward L. Ginzton Laboratory  
Stanford University  
Stanford, California 94305

## ABSTRACT

Several acoustic properties have been measured in an annealed round rolled bar of type 304 stainless steel. These properties were observed to depend upon both microstructure and the non-random crystal texture of this single phase, polycrystalline, face-centered cubic alloy. All measurements were made with longitudinal waves propagating parallel to the bar axis. The acoustic velocity was observed to be 0.3% higher near the outer surface than along the center of the bar, consistent with a stronger [111] texture in the outer fibers than at the center. The attenuation coefficient at the center was twice as large as at the outer surface. The measured difference in grain size at the center and surface was consistent with the observed attenuation difference. The acousto-elastic coefficient measured for a uniaxial tension stress applied along a bar diameter was at least 20% higher at the bar center than at its outer surface.

## INTRODUCTION

The acoustic properties of solid material depend on their microstructure. This paper describes efforts to correlate several acoustic properties with microstructural variations and preferred crystal texture in 304 stainless steel. Three acoustic properties were measured, longitudinal wave velocity, attenuation coefficient, and acousto-elastic constant.

## SPECIMEN MATERIAL

Type 304 stainless steel was chosen as a relatively simple, experimental convenient specimen material. 304 is the most common member of the austenitic, 18 chromium plus 8 nickel, family of stainless steels. The microstructure consists (ideally) of a single phase, face-centered cubic iron containing chromium and nickel in solution. The microstructure is an aggregate of many grains (crystallites). Figure 1 shows the specimen microstructure.

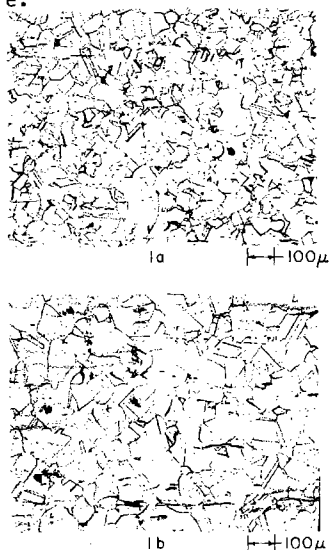


Fig. 1. Photomicrographs of the 304 stainless steel bar grain structure (a) at surface and (b) center radial position.

The specimen material was taken from a 76 mm diameter, rolled bar of 304 stainless steel. Flat acoustic test specimens 1.5 cm thick were cut transverse to and parallel to the bar axis, as shown in Fig. 2.

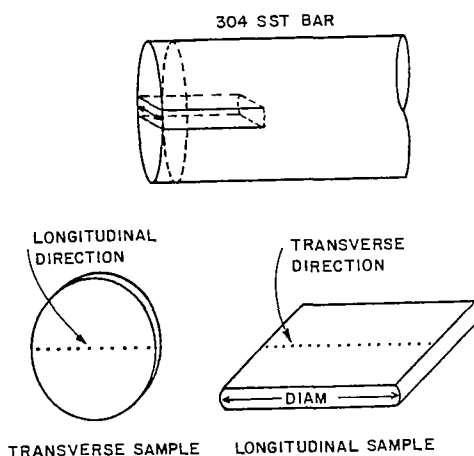


Fig. 2. Sample configuration for velocity and attenuation measurements.

In the as-received condition, the average grain size was about 100  $\mu\text{m}$ , but with a small size gradient from center to surface. The average grain diameter at the center was 120  $\mu\text{m}$ , and it decreased to 90  $\mu\text{m}$  at the surface. Grain size was determined by a mean intercept, lineal analysis. The reported average grain diameters are the true three-dimensional grain size. Average grain diameter is plotted in Fig. 3. The grain structure appeared perfectly equiaxed (no shape anisotropy).

To eliminate any effect of residual stresses possibly resulting from the steel manufacturing process, a transverse specimen of the bar stock was annealed at 1093°C for one hour, then air cooled. This caused a little grain growth. After annealing the center average grain size had increased to 128  $\mu\text{m}$ , while at the surface, no measurable grain growth had occurred. The annealed grain size is plotted in Fig. 3.

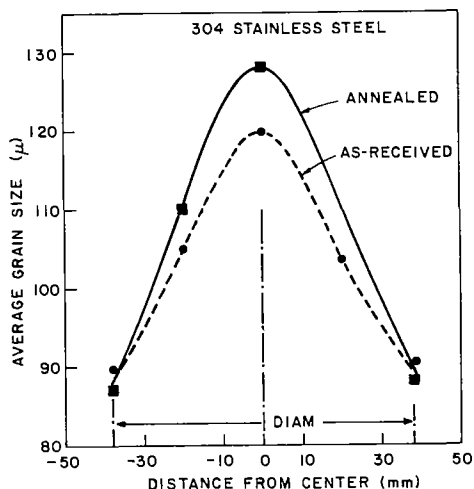


Fig. 3. Average grain diameter vs. radial position in 304 stainless steel as-received and annealed.

Although the grain structure gave no indication of anisotropy (directionality), some degree of preferred crystal orientation must have existed in this wrought 304 stainless steel bar. This is an unavoidable consequence of any plastic forming process. Rolling, wire drawing, extrusion, etc, invariably cause some non-randomness in the crystal orientation of the small grains comprising the polycrystalline microstructure. The degree of nonrandomness or preferred orientation depends on the material and its thermal-mechanical processing history. For face-centered cubic metals such as 304 stainless steel, we must expect some degree of [111], [100], or mixed [111] and [100] fiber texture. That is, a larger than random proportion of grains will be aligned with a [111] (cube diagonal) or a [100] (cube edge) crystal direction oriented close to the longitudinal axis of the bar (parallel to the rolling direction).

Any material property that depends on crystal orientation will be anisotropic in polycrystalline materials with preferred crystal texture. Acoustic velocity, depending directly on elastic constants, is directly affected by a preferred crystal texture, and it will be directionally dependent.

#### ACOUSTIC VELOCITY

The longitudinal acoustic wave velocity at 5 MHz was measured in the 304 stainless steel using a two-pulse echo system described elsewhere.<sup>1</sup> The accuracy of these measurements was better than  $\pm 0.02\%$ , being limited by the acoustic path length measurement (specimen thickness). The velocity was measured at different radial positions along bar diameters in both the transverse and longitudinally cut acoustic specimens. Figure 4 shows how the acoustic velocity, measured parallel to the rolling direction, varied with radial position in the as-received 304 stainless steel. The velocity was about 0.25% higher at the surface of the bar than at its center.

It is apparent that the pattern of velocity variation in the bar is approximately cylindrically symmetrical. Figure 5 shows an acoustical velocity

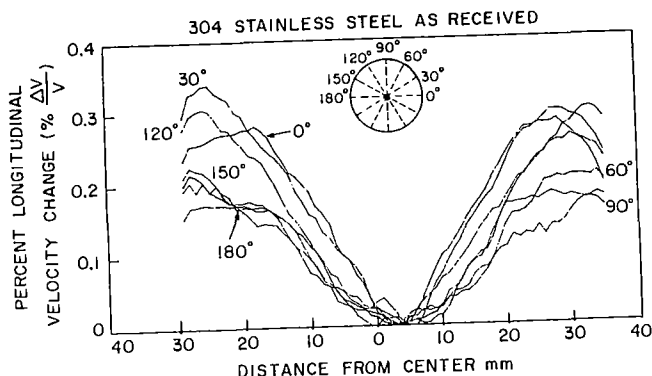


Fig. 4. Acoustic velocity scans along bar diameters in as-received 304 stainless steel. Velocity variation is normalized relative to the center of the bar.

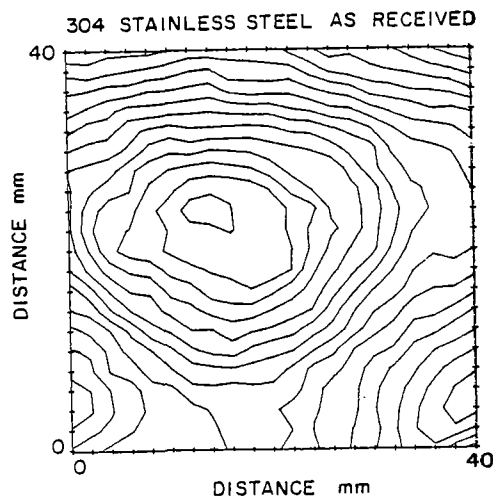
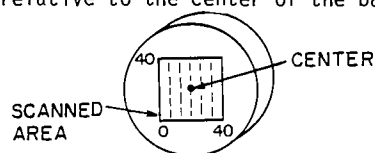


Fig. 5. Isovelocity contours on a cross section of rolled round bar of as-received 304 stainless steel.

scan of the center region of the transverse specimen; the isovelocity contours are roughly, but not perfectly, circular.

The acoustic velocity and its spatial pattern was practically identical in the annealed and as-received transverse specimens. In the longitudinally-cut specimen, the acoustic velocity was nearly independent of radial position, and was generally higher than in the transverse specimens. These measured velocities are plotted vs. position in Fig. 6.

In face-centered-cubic crystals, the longitudinal elastic constant is highest in [111] directions and lowest in [100] directions, therefore a [100] fiber texture will reduce the acoustic velocity in the direction of the fiber axis, while a [111] fiber texture will increase the longitudinal acoustic velocity in that direction. Comparison of the measured longitudinal acoustic

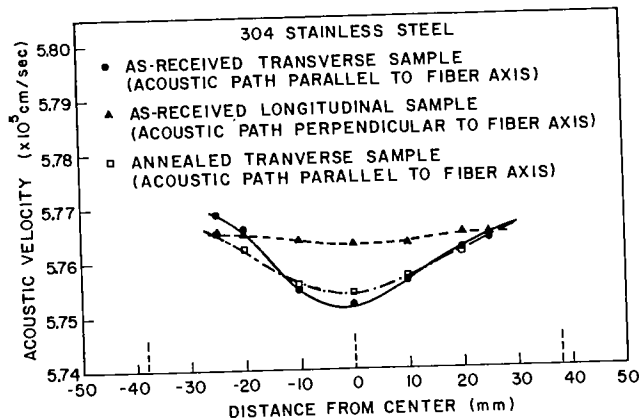


Fig. 6. Acoustic velocity measured at radial position in transverse and longitudinal samples.

velocity changes parallel to and perpendicular to the fiber axis, with the predicted influence on velocity by [100] and [111] fiber textures indicates that the ratio of the amount or strength of [111] fiber texture to [100] fiber texture,  $\gamma_{[111]}/\gamma_{[100]}$ , is largest at the surface and is smallest at the center. This could happen by the [100] texture strength decreasing from center to surface, by the [111] texture strength increasing from center to surface, or both.

#### CHARACTERIZATION OF TEXTURE BY X-RAY DIFFRACTION

An X-ray diffractometer was used to detect the kind and amount of texture in the 304 stainless steel bar and also to determine the variation of texture from the center to the surface of the round bar. The intensities of diffraction peaks were measured at different locations along the diameter in the as-received bars. The X-ray diffraction line intensities measured on specimens cut longitudinal or transverse to the bar axis are in proportion to the density of crystallites with the corresponding reflecting crystal planes oriented parallel to or transverse to the bar axis. (There is no (100) X-ray peak; the density of (100) planes is proportional to the (200) X-ray peak intensity.)

Comparison of the intensity of the (111) and (200) diffraction peaks at different locations along the diameter of the sample shows that the intensity of the (200) diffraction was stronger at the center and weaker away from the center toward the surface. Also, the intensity of (111) diffraction was stronger at the surface and weaker at the center for the transverse sample. In the longitudinal sample, the (111) peak intensity is uniform along the diameter of the sample, while the (200) peak was slightly stronger at the center than at the surface. A direct comparison of the intensities of the (111) and (200) diffraction peaks between longitudinal and transverse surface orientations would be of doubtful significance, because the differently oriented samples did not include the identical bar diameter. (The acoustic velocity scan suggested some deviation from perfect circular symmetry.) Table I shows the (100) and (200) X-ray diffraction peak intensities,  $I_{111}$ ,  $I_{200}$ , and the ratio of  $I_{111}/I_{200}$  along the diameter of the bar.

TABLE I

X-Ray Diffraction Peak Intensities  
(arbitrary units)

#### Longitudinal Sample

Position	$I_{200}$	$I_{111}$	$I_{111}/I_{200}$
surface	2.15	5.5	2.558
half	2.18	5.5	2.523
center	2.25	5.5	2.443

#### Transverse Sample

Position	$I_{200}$	$I_{111}$	$I_{111}/I_{200}$
surface	1.4	6.5	4.357
half	1.49	5.95	3.993
center	1.6	5.8	3.625

With [111] and [100] fiber textures, variations in the texture strength along the diameter should cause only minimal variation in peak intensities measured in the longitudinal specimen. However, when measured on the transverse specimen, the intensities should sensitively reflect variations in fiber texture strength. The ratio of (111) and (200) peak intensities was almost independent of radial position on the longitudinal sample, but varied considerably in the transverse specimen, as shown in Fig. 7. These X-ray data indicate that there is a duplex [111] + [100] fiber texture with the strength of the [111] component increasing from center to surface while the [100] component decreases from center to surface.

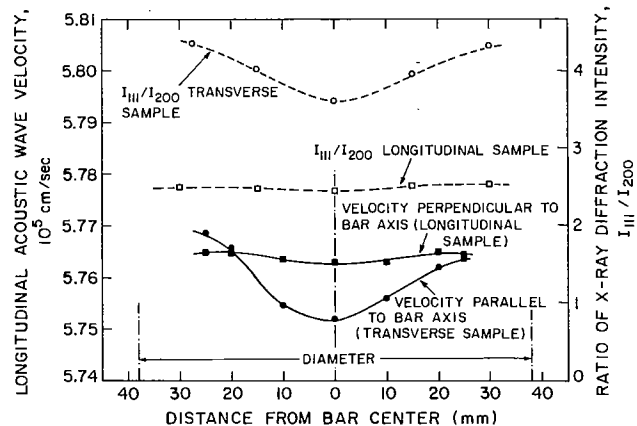


Fig. 7. X-ray line intensity ratio and acoustic velocity measured at varying radial positions in 304 stainless steel bar.

These X-ray data confirm the conclusion drawn from the acoustic velocity measurements that the ratio of [111] to [100] fiber texture increases from the center to the surface.

#### ATTENUATION MEASUREMENTS

In contrast to acoustic velocity, acoustic attenuation is strongly influenced by microstructure. As an acoustic plane wave passes through a medium, it dissipates energy by a variety of processes, and the wave amplitude decreases

accordingly. Letting  $U$  be the wave's displacement amplitude and  $x$  the acoustic path length:

$$U(x) = U_0 \exp(-\alpha x) \quad (1)$$

where  $U_0$  is the amplitude at  $x = 0$  and  $\alpha$  is the attenuation coefficient, usually expressed in dB per distance.

Attenuation measurements were made on the transverse cut acoustic specimens of the 304 stainless steel bar. Attenuation was measured at different radial positions to study the influence of grain size and preferred orientation. A three pulse-echo method was used with a 10 MHz broadband transducer.<sup>2</sup> The attenuation was measured from 5 to 10 MHz, corrected for diffraction, and plotted as a function of frequency. Figure 8 shows these data for the annealed sample; almost identical attenuation data were obtained from the as-received 304 stainless steel.

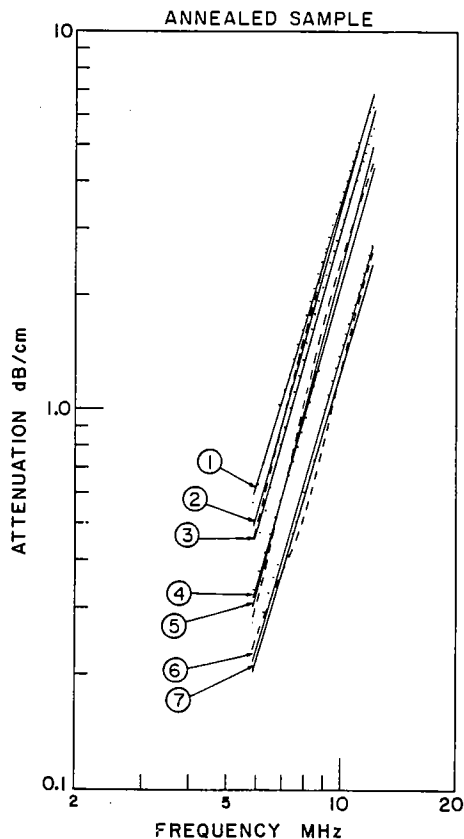


Fig. 8. Acoustic attenuation vs. frequency measured at various radial positions, (1) at the center, (2) and (3) 10 mm, (4) and (5) 20 mm, (6) and (7) 25 mm from the center in the annealed 304 stainless steel bar.

In the range of acoustic frequencies used, attenuation occurs predominantly by grain boundary scattering in single phase polycrystalline metals. When the wavelength of the propagating acoustic wave is much larger than the grain diameter, Rayleigh scattering is the predominant attenuation mechanism. In that case, the attenuation is expressed by

$$\alpha_R = S\mu^2\bar{D}^3f^4 \quad (2)$$

At higher frequencies when the wavelength becomes comparable to the grain diameter, the attenuation is controlled by stochastic scattering, expressed by

$$\alpha_S = S'\mu^2\bar{D}f^2 \quad (3)$$

In these two relations,  $\mu$  is the elastic anisotropy factor for each metal crystallite,  $\bar{D}$  is the average grain diameter,  $S$  and  $S'$  contain velocity terms, and  $f$  is the acoustic frequency.<sup>3</sup>

The attenuation vs. frequency data of Fig. 8 were fitted to an equation of the form

$$\alpha = Af^n \quad (4)$$

The frequency exponent,  $n$ , decreased from 4.0 at the surface to 3.44 at the center. This indicates that the acoustic attenuation occurred almost entirely by Rayleigh grain scattering. At the bar center, the  $n$  value of 3.44, indicating some stochastic scattering, is consistent with the larger grains at the center.

The attenuation was highest at the center position and decreased toward the surface. Figure 9 shows attenuation vs. radial position in the annealed 304 stainless steel as measured at three frequencies. This variation in attenuation with position was caused by the gradient in grain size from center to surface.

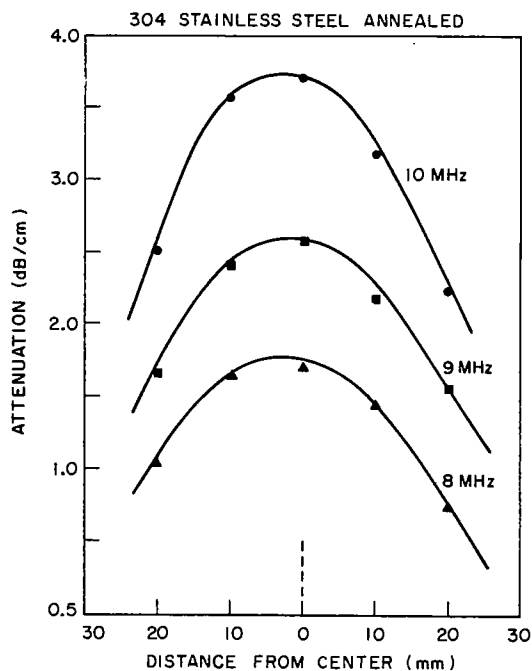


Fig. 9. Acoustic attenuation coefficient vs. radial position in the annealed 304 stainless steel.

## ACOUSTOELASTIC EFFECT

Because the elastic constants of materials are not quite independent of the state of elastic stress, acoustic wave velocity depends on the state of static stress of the acoustic medium. This manifestation of nonlinear elasticity, the acousto-elastic effect, provides the basis for acoustic nondestructive stress measurement. For example, in an elastically isotropic solid in a state of plane stress, the longitudinal acoustic velocity perpendicular to the stress plane is linearly proportional to the static stress amplitude:

$$V_{\sigma} = V_0 + V_0 B(\sigma_x + \sigma_y) \quad (5)$$

or

$$\frac{\Delta V}{V} = \frac{(V_{\sigma} - V_0)}{V_0} = B(\sigma_x + \sigma_y) \quad (6)$$

where  $V_{\sigma}$  and  $V_0$  are the acoustic velocity in the stressed and unstressed states,  $\sigma_x$  and  $\sigma_y$  are the principal values of the static stress, and  $B$  is an acousto-elastic coefficient, an elastic property of the material:

$$B = \frac{\mu\lambda - \lambda(m + \lambda + 2\mu)}{\mu(\lambda + 2\mu)(3\lambda + 2\mu)} \quad (7)$$

where  $\lambda$  and  $\mu$  are the familiar Lamé linear elastic constants, while  $\lambda$  and  $m$  are two of the three third order Murnaghan nonlinear isotropic elastic constants. Other, similarly constituted, acousto-elastic constants are appropriate for other stress geometries, shear waves, etc. In principle, the relative change in acoustic velocity is linearly proportional to stress, and the acousto-elastic constant of proportionality, such as  $B$ , is a simple isotropic property of the material; in reality, it is not.

One difficulty complicating the development of practical acousto-elastic stress measurements is the variability and anisotropy of the acousto-elastic coefficients. An example of variations that occur in the acousto-elastic coefficient  $B$  was observed with the 304 stainless steel bar described above.

A piece was removed from the 76 mm diameter round bar, as depicted in Fig. 10. Pin grip end pieces were welded onto the stainless steel sample so that a tensile stress could be applied; the stress axis coincided with a diameter of the original bar stock. After welding, the sample was annealed at 1100°C for one hour to remove residual stress. The acoustic velocity of longitudinal acoustic waves was measured along the gauge section of the composite tension test specimen at different values of applied tensile stress. From those data, the acousto-elastic coefficient  $B$  was obtained as a function of radial position in the 304 stainless steel bar. Figure 11 shows  $B$  as a function of radial position.

The pronounced variation in the acousto-elastic coefficient plotted in Figure 11

## 304 STAINLESS STEEL SAMPLE

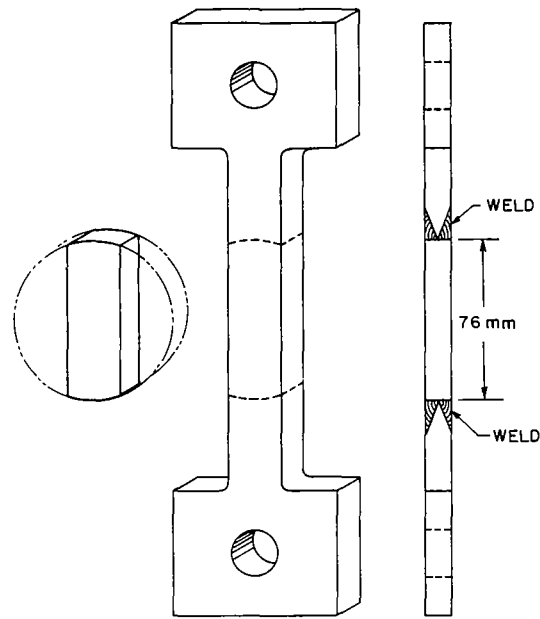


Fig. 10. Tension test specimen constructed from 304 stainless steel bar to measure acoustoelastic coefficient.

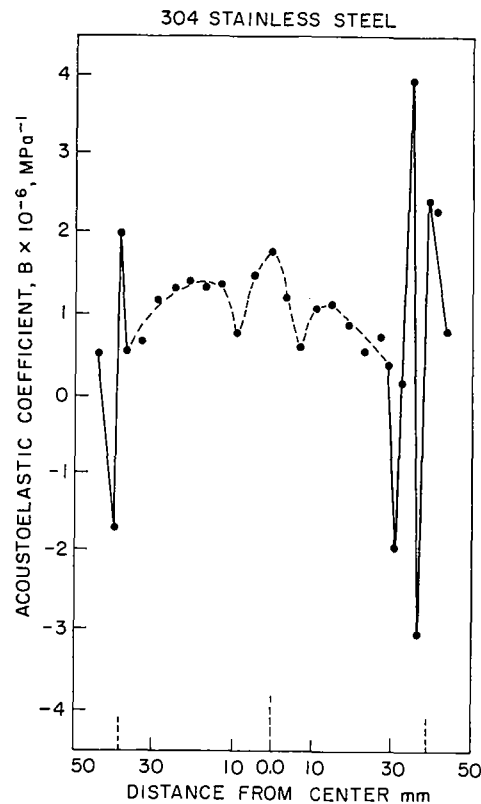


Fig. 11. Acoustoelastic coefficient vs. radial position in 304 stainless steel bar.

can be related to the radially-varying fiber texture discussed in connection with acoustic velocity measurements and to the welds used to construct the specimen. The wild fluctuations in  $B$  values measured 30 mm and farther from the

original center line of the round bar occur in the welds (weld material is also 304 stainless steel). Between the welds, the measured B values are highest at the center line and are lower toward the outer surface of the bar. This variation is consistent with the radially-varying fiber texture pattern observed in the bar. The fine scale variation in B near the center of the bar is not understood. Possibly it may reflect fine scale variations in the texture. The acoustic measurements were made using an acoustic beam 1.5 mm in diameter capable of spatially resolving the plotted fine scale B variations.

While explanations for the variability encountered in measuring acousto-elastic coefficients are incomplete and necessarily tentative, it is clear that large variations do occur even from point to point in the same piece of material. Such variations must be better understood if the full potential of acousto-elastic stress measurements is to be achieved.

#### SUMMARY

The acoustic properties of a bar of 304 stainless steel were observed to depend upon position and orientation in a manner coincident with the variation of grain size and preferred crystal texture in the bar. Acoustic velocity was demonstrated to be a sensitive measure of preferred texture and acoustic attenuation could be correlated with small variations in grain size. The acousto-elastic coefficient exhibited a position dependence apparently related to local variations in preferred texture.

#### ACKNOWLEDGMENT

The work described in this paper was performed as part of a research program on acoustic nondestructive testing sponsored by the Air Force Office of Scientific Research, Contract No. F49620-79-C-0217.

#### REFERENCES

1. D. B. Ilıc, G. S. Kino, and A. R. Selfridge, Rev. Sci. Instr., 50 (17), 1527-1531 (1979).
2. N. Grayeli, D. B. Ilıc, F. Stanke, G. S. Kino, and J. C. Shyne, Proceedings of the DARPA/AFML Review of Progress in Quantitative NDE, 429-434, (1980).
3. I. M. Lifshits and G. D. Parkhomovskii, Zhur-EKSP-iteoret., Fiz, 20, 175 (1950).

## SUMMARY DISCUSSION

William Pardee, Chairman (Rockwell Science Center): Are there any questions?

Unidentified Speaker: What was the slope of your attenuation, what was the power, and what was the frequency?

Frederick Stanke (Stanford University): The power slope varied between the curves I showed you, between 3.5 and -4. The highest was 3.9. For this sample, the slope of the attenuation was somewhat lower in the center of the sample. That is what we would expect because the grains are larger so the Rayleigh approximation is not as good. At the outside of the sample where the grains are smaller, it approached up to the fourth.

Unidentified Speaker: Can you take into account any sort of damping with dislocation, and would that be affected by an annealing?

Frederick Stanke: Yes. What I have described is simply a measurement system. We have measured the attenuation, and our job now is to interpret what that attenuation comes from, and theory needs to be done. Dislocation attenuation hasn't been something that we have looked into a lot. I was under the impression that the level would be much lower than what we're measuring.